ISSN 0208-7774 TRIBOLOGIA 3/2022 p. 17–24
DOI: 10.5604/01.3001.0016.1020

Barbara KALANDYK[*], Renata ZAPAŁA[**], Monika MADEJ[***], Justyna KASIŃSKA[****], Katarzyna PIOTROWSKA[*****]

INFLUENCE OF PRE-HARDENED GX120Mn13 CAST STEEL ON THE TRIBOLOGICAL PROPERTIES UNDER TECHNICALLY DRY FRICTION

WPŁYW WSTĘPNEGO UTWARDZENIA STALIWA GX120Mn13 NA JEGO WŁAŚCIWOŚCI TRIBOLOGICZNE W WARUNKACH TARCIA TECHNICZNIE SUCHEGO

Key words: high manganese cast steel, hardness, wear resistance, ball-on-disc test.

Abstract: This paper presents the results of tribological tests on high manganese GX120Mn13 cast steel under technically dry friction conditions. The tests were carried out using a TRB^3 ball-on-disc tribometer using a 6mm-diameter SiC ball as a counter-sample for a specimen made of GX120Mn13 cast steel containing a localised pre-hardening area on the test surface with a hardness of approximately 597 HV_{10} (the non-hardened area had a hardness of approximately 325–364 HV_{10}). During the test, the ball travelled in a 16.68 mm diameter circle and passed through both hardening and non-hardened areas. The resulting erosion marks were assessed using an optical profilometer and scanning microscope tests, which showed that the maximum depth of erosion in the previously hardening area was 0.77 μm and was more than twice as deep as in the non-hardened areas surveyed. In contrast, the area of attrition was twice as small as in the non-hardened area located in the axis of the previously applied load and more than three times smaller, but in the area located on the side of the axis and 8.34 mm away from it. Thus, from the point of view of the abrasion resistance of GX120Mn13 cast steel, the validity of its prior hardening before the operation was confirmed.

Słowa kluczowe: staliwo wysokomanganowe, twardość, odporność na zużycie, test ball-on-disc.

Streszczenie: W artykule przedstawiono wyniki badań tribologicznych wysokomanganowego staliwa GX120Mn13 w warunkach tarcia technicznie suchego. Badania przeprowadzono przy użyciu tribometru TRB^3 typu ball–on–disc stosując jako przeciwpróbkę kulkę z SiC o średnicy 6mm dla próbki wykonanej ze staliwa GX120Mn13 zawierającej na powierzchni badanej lokalny obszar wcześniej umocniony o twardości ok. 597 HV_{10} (obszar nieumocniony posiadał twardość ok 325–364 HV_{10}). Kulka w czasie testu poruszała się po okręgu o średnicy 16.68 mm i przechodziła zarówno przez obszar umocniony, jak i nieumocniony. Otrzymane ślady wytarcia oceniano za pomocą badań wykonanych na profilometrze optycznym i mikroskopie skaningowym. Na podstawie przeprowadzonych badań wykazano, że w obszarze wcześniej umocnionym maksymalna głębokość wytarcia wynosiła 0.77 μm i była ponad dwukrotnie mniejsza niż w badanych obszarach nieumocnionych. Z kolei pole wytarcia było dwukrotnie mniejsze niż w obszarze nieumocnionym, znajdującym się w osi przyłożonego wcześniej obciążenia i ponad trzykrotnie mniejsze w porównaniu z obszarem znajdującym się z boku osi i oddalonym od niej o 8.34 mm. Tym samym, z punktu widzenia odporności na zużycie ścierne staliwa GX120Mn13, potwierdzono słuszność jego wcześniejszego umocnienia przed eksploatacją.

[*] ORCID: 0000-0002-4604-0281. AGH University of Science and Technology, Faculty of Foundry Engineering, Reymonta Street 23, 30-059 Krakow, Poland.
[**] ORCID: 0000-0002-7634-8316. AGH University of Science and Technology, Faculty of Foundry Engineering, Reymonta Street 23, 30-059 Krakow, Poland.
[***] ORCID: 0000-0001-9892-9181. Kielce University of Technology, Faculty of Mechatronics and Mechanical Engineering, Tysiąclecia Państwa Polskiego 7 Ave., 25-314 Kielce, Poland.
[****] ORCID: 0000-0002-2225-0639. Kielce University of Technology, Faculty of Mechatronics and Mechanical Engineering, Tysiąclecia Państwa Polskiego 7 Ave., 25-314 Kielce, Poland.
[*****] ORCID: 0000-0001-6366-2755. Kielce University of Technology, Faculty of Mechatronics and Mechanical Engineering, Tysiąclecia Państwa Polskiego 7 Ave., 25-314 Kielce, Poland.

INTRODUCTION

For many years, high manganese GX120Mn13 cast steel has been one of the materials with very attractive performance properties that make castings made from this material applicable in harsh operating conditions, mainly in the mining and railway sectors **[L. 1–4]**. What distinguishes this grade of cast steel from wear-resistant alloys is the surface hardening as a result of twinning and slip (while the rest of the casting remains ductile) occurring under high stresses and impact loads during operation of, for example, railway turnouts, crushers or coal mills **[L. 2, 5–7]**. In the case of many castings, especially those operating, for example, in crushers, in addition to high impact pressures, there are much lower pressures from the already crushed ground material. The impact of that material is insufficient to strengthen the surface of the casting and poses a greater threat to its dimensional stability. For this reason, much research has been devoted to the hardened of the cast Hadfield steel matrix by particles, e.g., Ti, V primary carbides **[L. 8–10]** or by prior hardened of the surface layer (nanocrystalline hardened of the surface layers) by techniques such as burnishing or shock wave **[L. 6, 11, 12]**. High-manganese cast steel grades up to about 1.5% Cr are also known. This element is introduced to increase the hardness of the steel matrix and high manganese cast steel, thereby influencing changes in the type of wear **[L. 13, 14]**. In addition to Cr, Ti or V is often introduced only because the wear resistance of this material depends on a combination of hardness, strength, ductility and operating conditions. The research undertaken in this paper aimed to determine the influence of hardening GX120Mn13 cast steel on tribological properties under technically dry friction conditions. The issue of hardening the surface layer by crushing and increasing abrasion wear resistance has been the subject of many studies **[L. 7, 15]**. However, the friction pair of GX120Mn13 Hadfield cast steel and SiC has not been investigated to date. In the paper presented here, indicators in the form of depth, width and area of abrasion were used to describe wear.

MATERIALS AND METHODS

The test were carried out using high manganese cast steel with the following chemical composition: 1.0% C, 11.5% Mn, 0.6% Si, 0.9% Cr, 0.05% P, 0.01% S, 0.07% Mo, 0.25% Ni. A suitably machined specimen measuring 85x25x20 mm was force-loaded while maintaining a uniaxial stress state in a plane perpendicular to the specimen surface. The direction of the applied multiple loads caused deformation in the areas directly in contact with the load, probably resulting from activated multiple twinning and slip. The lateral surface of the specimen (perpendicular to the force's application) was ground to produce a visible hardening area due to the applied load. The sample thus prepared, with a roughness of less than 0.2 μm (R_a), was subjected to wear resistance tests. Prior to the test, the surface of the cast steel was sanded on sandpaper with a gradation of 220, 400, 800 and 1,200. Tribological tests were carried out under technically dry friction conditions at room temperature on an Anton Paar TRB3 tribotester using the ball-on-disc method. The counter-sample was a ball made of SiC with a diameter of 6 mm, and the sample was a cuboid measuring 45x25x20 mm. **Figure 1** shows a view of the friction pair, and the test parameters are summarised in **Table 1**. The tribological properties of the friction pair under study were assessed on the basis of changes in the coefficient of friction and microscopic observations of the surface of wear marks in the hardened and non-hardened areas. The SGS examination was carried out using a Leica DCM8 confocal microscope with interferometric mode. Using confocal mode, a 1.2x1.6 mm area was measured at 20x magnification. These

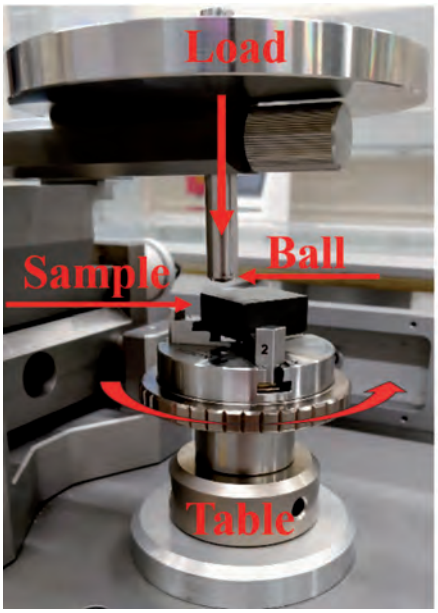

Fig. 1. Friction pair
Rys. 1. Widok węzła tarcia

measurements made it possible to determine the surface profiles from which the depth and width of the abrasion were measured, which in turn allows for determining the wear mark area. Surface abrasion marks in the hardened and non-hardened areas were also investigated using a JEOL 5500LV scanning electron microscope equipped with an IXRF's EDS system for X-ray microanalysis. In addition, the hardness of the material was tested using the Vickers method at 10 N and 0.1 N load, using Innovatest's Nexus 4000 hardness tester and Anton Paar's MHT^3 microhardness tester. Five measurements were taken for each of the methods presented above.

Table 1. Conditions for tribological test
Tabela 1. Parametry testu tribologicznego

Temperature T /°C	Types of balls	Diameter of balls d / mm	Normal load F_n / N	Friction track diameter r / mm	Sliding speed v / m/s	Total sliding distance L / m	Test duration t / s
25±1	SiC	6	10	16.68	0.1	1,000	9,891.14

RESULTS AND ANALYSIS

The hardness of test material in hardening and non-hardened areas

Hardness tests performed on both the MCT^3 microhardness tester and the Nexus 4000 indicate that hardness decreased with increasing distance from the hardened surface. In the case of instrumental hardness, the parameter was tested on a 4 mm section. In the surface layers in direct contact with the applied load, the microhardness of the austenitic matrix was approximately 900 $HV_{0.1}$, which was 50% higher compared to the non-hardened surface. This is related to the higher dislocation density in this area [**L. 7**]. At a distance of approximately 1 mm from the hardened surface, the matrix hardness decreased to 500 $HV_{0.1}$; at a distance of 2 mm, the hardness was approximately 450 $HV_{0.1}$.

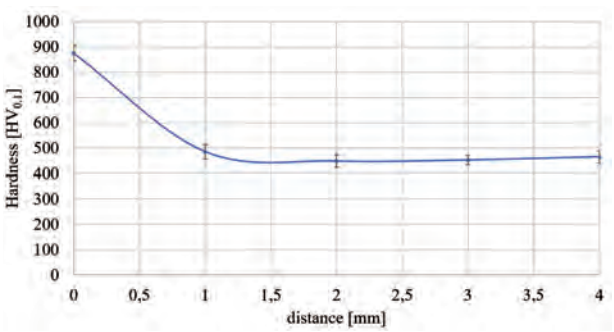

Fig. 2. Change in the microhardness of the matrix of the steel under test in the hardened area
Rys. 2. Zmiana mikrotwardości osnowy badanego staliwa w obszarze umocnionym

Such a hardness value was also obtained at distances of 3 and 4 mm, thus indicating a stabilisation of hardness in the hardened area (**Fig. 2**).

In turn, the hardness results in the hardened and non-hardened areas are summarised in **Table 2**, and the location of the measurement points is shown in **Figure 3**.

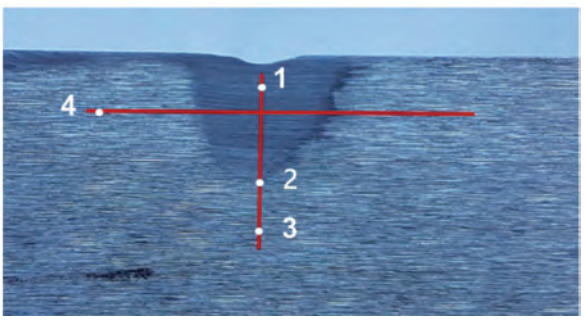

Fig. 3. Marked areas of the hardness measurement; the dark area is the area of plastic deformation under applied load
Rys. 3. Zaznaczone miejsca pomiaru twardości, ciemny obszar to obszar odkształcenia plastycznego pod wpływem przyłożonego obciążenia

Table 2. The hardness of the cast steel
Tabela 2. Twardość badanego staliwa w obszarze badań

Area of measurement	Average hardness, HV_{10}	Standard deviation
1	597	3.61
2	386	3.79
3	364	4.04
4	325	3.46

The hardness of materials is one of the determining factors in friction and wear. As hardness increases, the coefficient of friction and wear decreases. The results above allow us to predict that wear in the hardened area will be considerably less than outside.

Ball-on-disc test

Tribological tests were carried out in such a way that the ball passed through a hardened and non-hardened area during the test. The location on the test sample of the path followed by the counter-sample is shown in **Figure 4**. The hardened area of the sample is marked with a square, while points 1, 3 and 4 mark the areas where the wear profiles were tested. Points 1 and 3 are on the axis of the applied load, while point 4 is outside it. The weight of the sample before the test was 169.0775 g and 169.0764 g after the test (it decreased by 0.0011 g), while the weight of the ball did not change. Thus, there was no material transfer between the bead and the test material sample. This can probably be attributed to the high hardness of SiC of approximately 1150 HB.

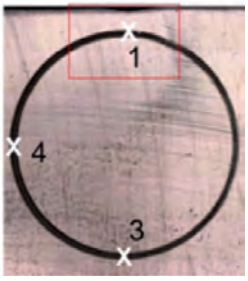

Fig. 4. Diagram of areas in which wear profiles were recorded in the box, the area plastically deformed due to applied load 1, the area in the axis of impact outside the area of hardening 3, the area on the side outside the hardening 4

Rys. 4. Schemat obszarów, w których rejestrowano profile zużycia, w ramce obszar odkształcony plastycznie na skutek przyłożonego obciążenia 1, obszar w osi uderzenia poza obszarem umocnienia 3, obszar z boku poza umocnieniem 4

Figure 5 shows the dependence of the coefficient of friction as a function of distance, from which it can be seen that the coefficient of friction for the test material stabilises after approximately 500 m and ranges between 0.4 and 0.58.

The tribological test parameters determine the friction coefficient values in the fortified and non-hardened zones, so a combined graph is presented below. In the next research stage, it was planned

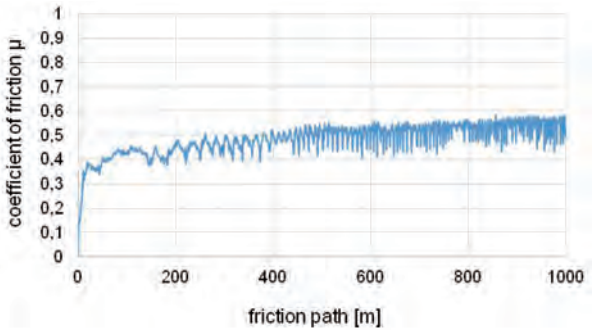

Fig. 5. Coefficient of friction

Rys. 5. Wartości współczynnika tarcia μ w funkcji drogi tarcia

to carry out tests in a circular (curved) motion to determine the friction coefficient values in the hardened or non-hardened area only.

The surface texture, surface profiles, and an indication of the depth, width and surface area of the abrasion marks of the tested cast steel in areas 1, 3 and 4 are shown in **Figures 6–7**. The images provided show a clear difference between the wear track surface profiles and the indicators in areas 1 and 3, and 4.

Observations of the surface topography and wear track on non-hardened surfaces (3 and 4) indicate the presence of characteristic furrows, most likely caused by the loose rolling of hard particles originating from the matrix – from chromium carbides/ or non-metallic inclusions in the area of the friction area. In the case of the hardened surface, such deep furrows were not observed.

Based on microscopic observations of the wear marks, it was found that the smallest abrasion depth and abrasion area were located at the surface where the load was applied, i.e., in the plastically deformed and hardened areas. In contrast, the values of the recorded parameters increase in area 3 compared to area 1. In areas 3 and 4, the depth of abrasion is more than doubled, while the abrasion area has increased from 100.5 μm^2 to 232.2 μm^2 in area 3 and to 362.7 μm^2 in area 4.

Microstructure of the wear track

A study of the surface topography of the wear track after the tribological tests carried out using SEM-EDS scanning microscopy indicates an abrasive surface degradation/wear mechanism. The irregularities observed on the abrasion marks, in the form of scratches and furrows, are of a linear nature oriented according to the movement of the counter-sample occurring during the test (**Fig. 8**).

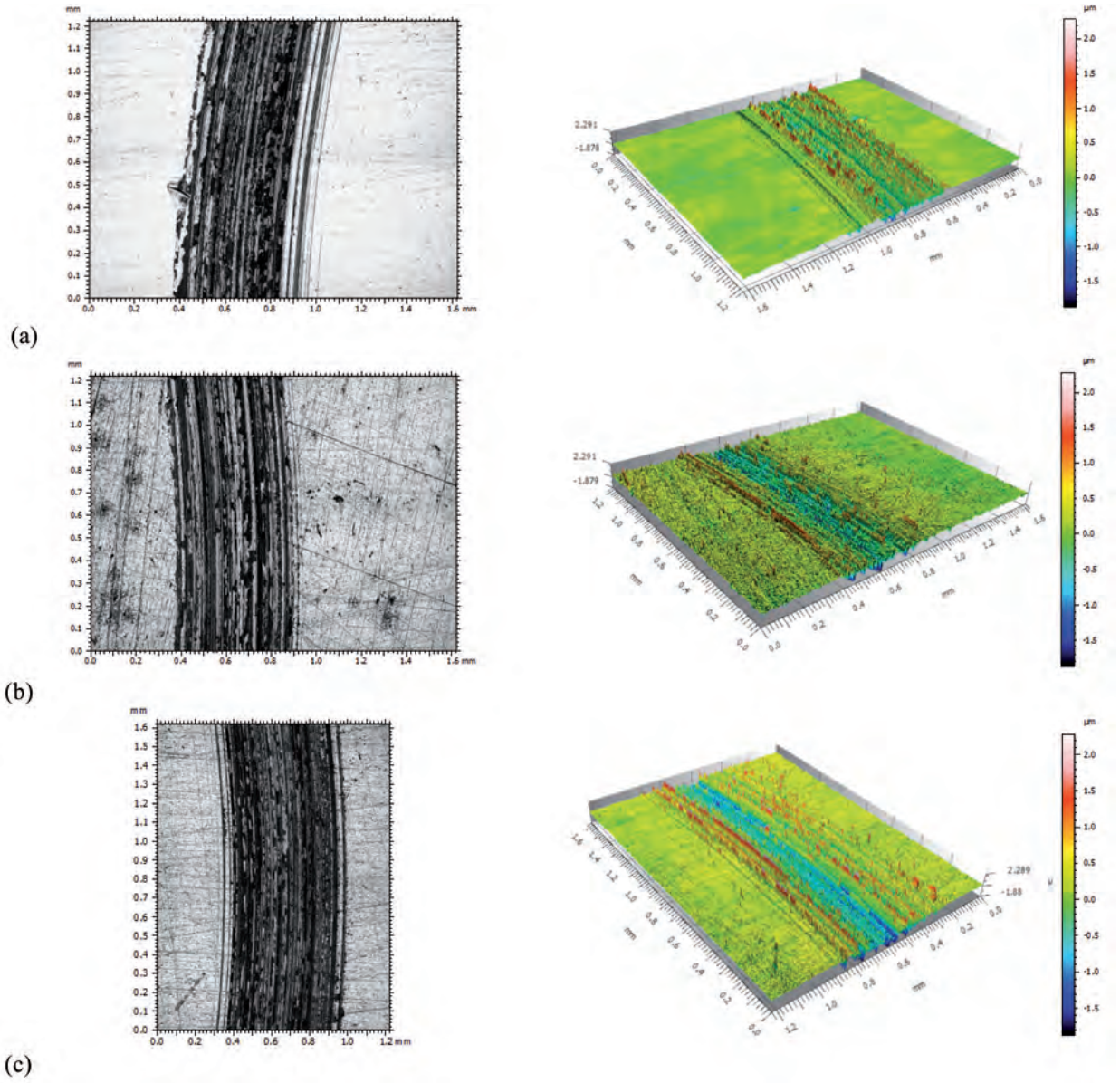

Fig. 6. Topography of the surface of the 2D and 3D cast steel wear marks in the areas examined: area 1 hardening at the surface (a), area 3 located in the axis of impact outside the area of hardening (b), area 4 located on the side outside the hardening (c)

Rys. 6. Topografia powierzchni śladów wytarcia 2D i 3D staliwa w badanych obszarach: obszar 1 umocniony przy powierzchni (a), obszar 3 znajdujący się w osi uderzenia poza obszarem umocnienia (b), obszar 4 znajdujący się z boku poza umocnieniem (c)

Observations carried out using magnifications in the 4000-5000x range revealed typical surface defects in the form of microcracks and chipping in the areas of abrasion marks [**L. 16]**. Deposited particles were observed in some micro-areas (**Figures 9–10**). All areas of the abrasion mark showed cavities formed after the chipping of hard particles from the matrix of the test material, probably from Cr carbides or non-metallic inclusions. The EDS analysis showed enrichment of areas with visible precipitates in oxygen, Si (7.3%) and Mn (5.9%) (**Fig. 10**), which may indicate that oxidation processes occur during friction **[L. 17].**

The SEM-EDS tests carried out did not show a significant difference in the abrasion marks between the pre-hardened and non-hardened areas tested. In the zone of frictional contact between the SiC ball and the tested cast steel in areas 1, 3 and 4, cracks and furrows correspond to the direction of movement that occurred during the test.

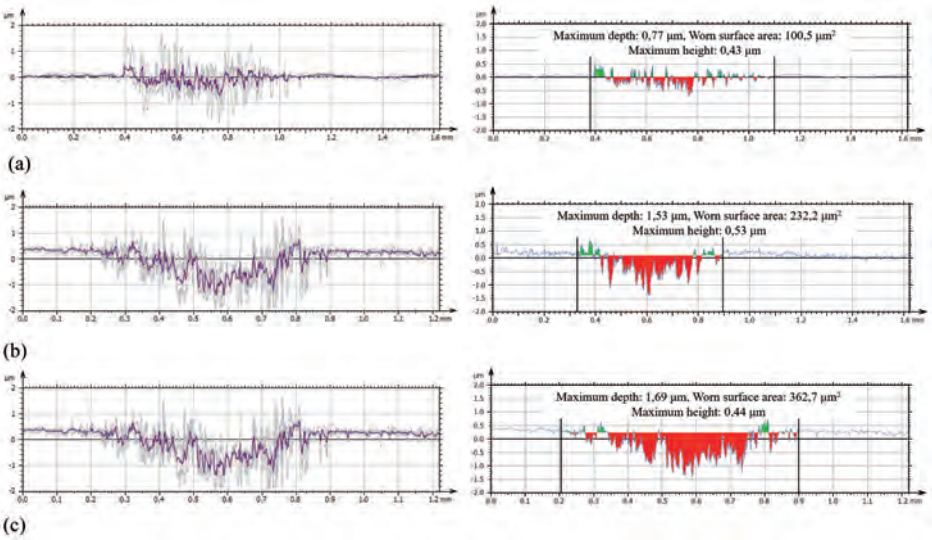

Fig. 7. Surface profiles on the cross-section in the areas examined: area 1 hardened at the surface (a), area 3 located in the axis of impact outside the area of hardening (b), area 4 located on the side outside the hardening (c)

Rys. 7. Profile powierzchni na przekroju poprzecznym w badanych obszarach: obszar 1 umocniony przy powierzchni (a), obszar 3 znajdujący się w osi uderzenia poza obszarem umocnienia (b), obszar 4 znajdujący się z boku poza umocnieniem (c)

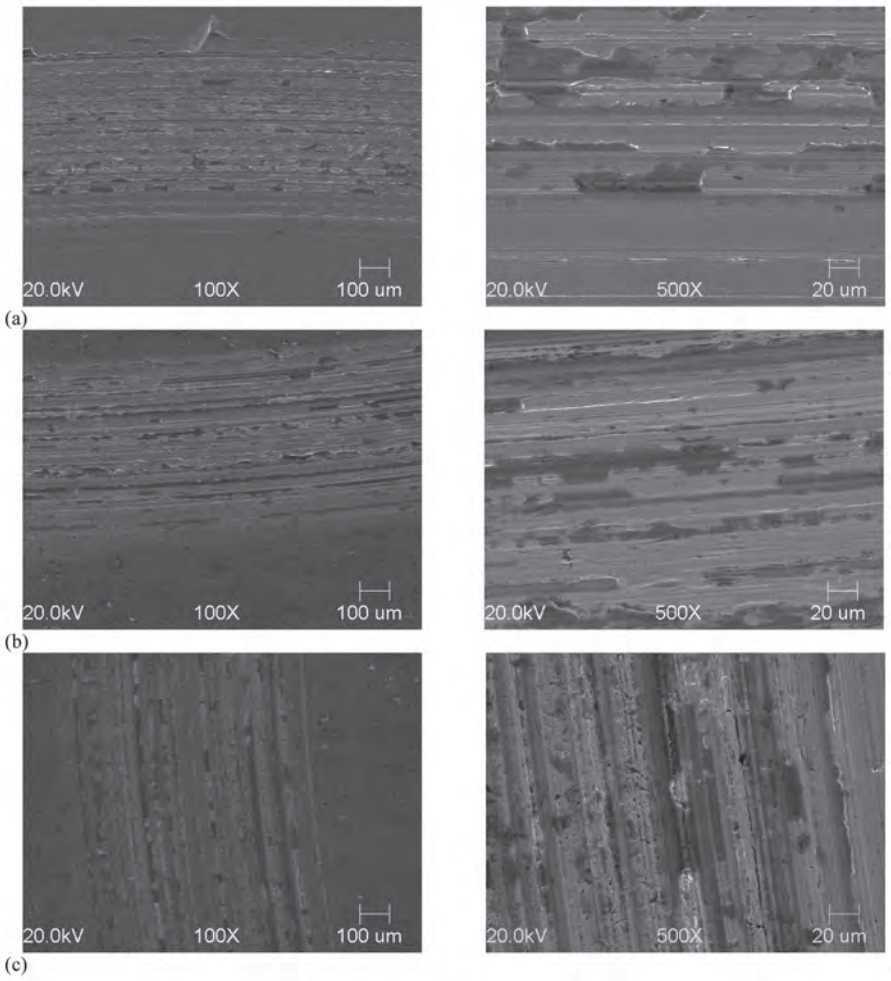

Fig. 8. SEM images of abrasion marks in the areas examined, a – area 1 hardening near the surface, b – area 3 located in the axis of impact outside the hardening, c – area 4 located on the side outside the hardening

Rys. 8. Obrazy SEM śladów wytarcia w badanych obszarach, a – obszar 1 umocniony przy powierzchni, b – obszar 3 znajdujący się w osi uderzenia poza obszarem umocnienia, c – obszar 4 znajdujący się z boku poza umocnieniem

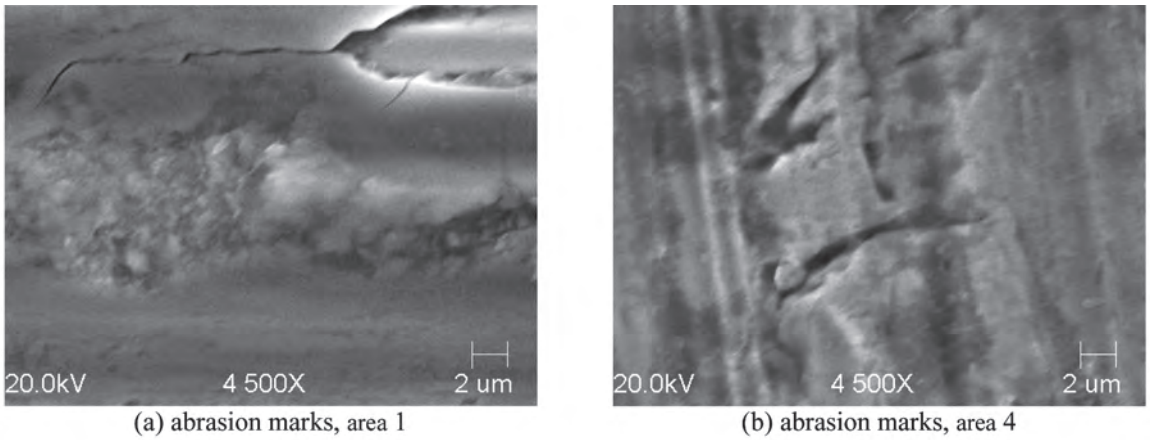

Fig. 9. Images of microcracks on abrasion marks
Rys. 9. Obrazy mikropęknięć na śladach wytarcia

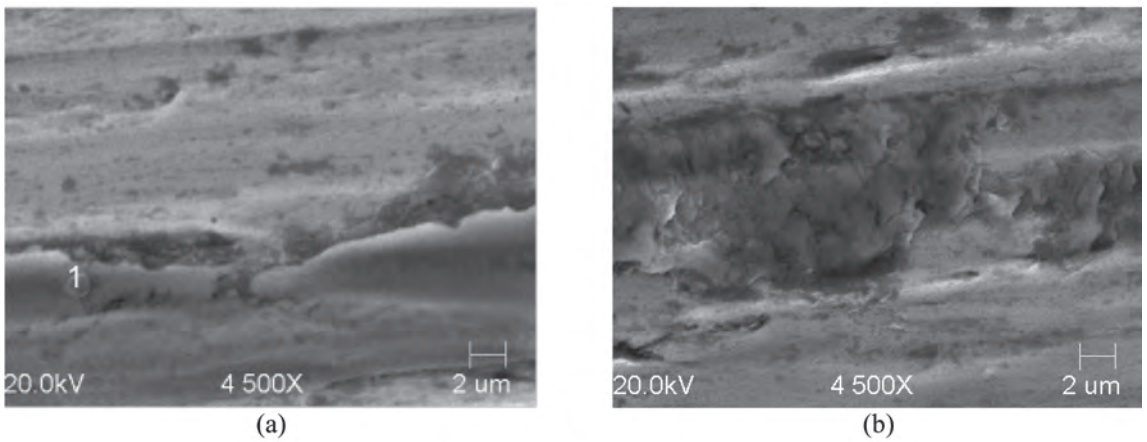

Fig. 10. The surface area of the abrasion mark with visible local cavities of chipped particles (a) on flat surfaces of the marks, (b) in furrows with visible precipitates
Rys. 10. Obszar powierzchni śladu wytarcia z widocznymi lokalnymi ubytkami po wykruszonych cząstkach (a) na płaskich powierzchniach śladów, (b) w bruzdach z widocznymi wydzieleniami

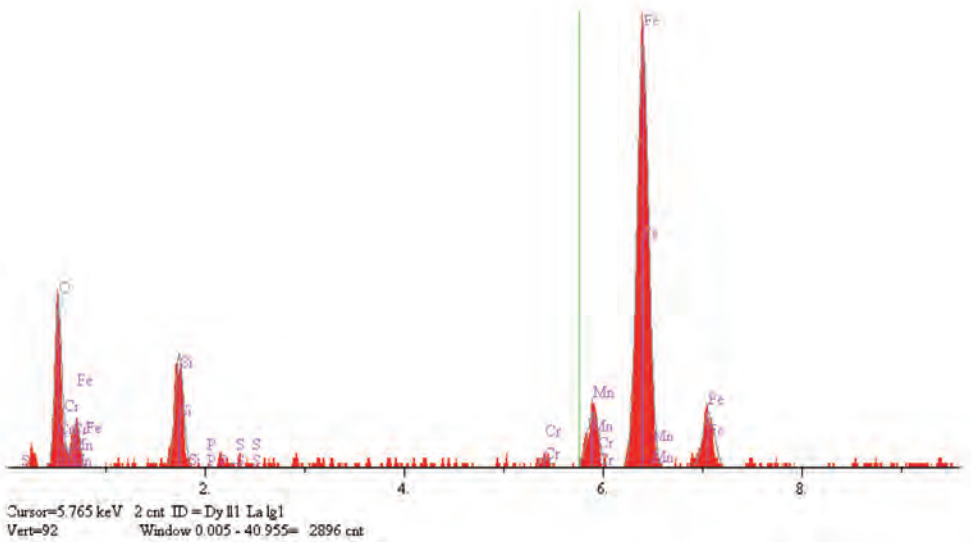

Fig. 11. Example of spectrum from point 1 in Fig. 10a
Rys. 11. Przykład widma z punktu 1 z rys. 10a

CONCLUSIONS

The results confirm the beneficial influence of pre-hardening of GX120Mn13 cast steel on hardness and tribological wear resistance under technically dry friction conditions. The hardness measurements' differences are due to the use of different weights and types of indenters. Research into the impact of the type of testing device and indenter type will be the subject of future studies. The micro-areas of the surface of the abrasion marks showed cracks and chipping marks of particles present in the matrix, probably from Cr carbides, and the presence of oxide inclusions in the slots of the furrows.

REFERENCES

1. Smith R.W., De Monte A., Mackay W.B.F.: Development of high-manganese steels for heavy duty cast-to-shape applications. Journal of Materials Processing Technology. 2004, 153–154, pp. 589–595.
2. Głownia J.: Odlewy ze stali stopowej – zastosowanie. Fotobit, Kraków 2002.
3. Dastur Y.N., Leslie W.C.: Mechanism of work hardening in Hadfield manganese steel. Metallurgical Transactions A. 1981. 12A, pp. 749–759.
4. Kalandyk B., Zapała R.: Effect of high-manganese cast steel strain hardening on the abrasion wear resistance in a mixture of SiC and water. Archives of Foundry Engineering. 2013, 13, 4, pp. 63–66.
5. Krawczyk J., Matusiewicz P., Frocisz Ł., Augustyn-Nadzieja J., Parzycha S.: The wear mechanism of mill beaters for coal grinding made-up from high manganese cast. 73 WFC Kraków 2018: "Creative Foundry", pp. 213–214.
6. Stradomski Z.: The role of microstructure in the wear behaviour of abrasion-resistant cast steels. Wyd. Politechniki Częstochowskiej, Częstochowa 2010.
7. Kalandyk B., Zapała R., Kasińska J., Madej M.: Evaluation of microstructure and tribological properties of GX120Mn13 and GX120MnCr18-2 cast steels. Archives of Foundry Engineering. 2021, 21, 4, pp. 67–76.
8. Quan Shan, Ru Ge, Zulai Li, Zaifeng Zhou, Yehua Jiang, Yun-Soo Lee, Hong Wu.: Wear properties of high-manganese steel strengthened with nano-sized V2C precipitates. Wear. 2021, 15, pp. 482–483.
9. Mahlami C.S., Pan X.: Mechanical properties and microstructure evaluation of high manganese steel alloyed with vanadium. Retrieved August 10, 2021, from https://doi.org/10.1063/1.4990236.
10. Quan Shan, Ru Ge, Zulai Li, Zaifeng Zhou, Yehua Jiang, Yun-Soo Lee, Hong Wu.: Wear properties of high-manganese steel strengthened with nano-sized V2C precipitates. Wear. 2021, pp. 482–483.
11. Stradomski Z., Morgiel J., Olszewski J.: Significance of dislocations in the mechanism of Hadfield cast steel strengthening. Inżynieria Materiałowa. 1999, 5, pp. 398-401.
12. Kosturek R., Maranda A., Senderowski C., Zasada D.: Research into the application of explosive welding of metal sheets with Hadfield's steel (Mangalloy). High-Energetic Materials. 2016, 8, pp. 91–102.
13. Sobula S., Tęcza G.: Stabilisation of the Hadfield cast steel microstructure at increased temperatures in the presence of chromium. Przegląd Odlewnictwa. 2009, 3, pp. 22–27.
14. Krawczyk J., Bembenek M., Pawlik J.: The role of chemical composition of high-manganese cast steels on wear of excavating chain in railway shoulder bed ballast cleaning machine. Materials. 2021 16, 14 (24).
15. Krawiarz J., Magalas L.: Modificated Hadfield-cast steel with increased wear resistance. Przegląd Odlewnictwa. 2005, 55, pp. 666–672.
16. Niemczewska-Wójcik M., Wójcik A.: The multi-scale analysis of ceramic surface topography created in abrasive machining process. Measurement. 2020, 166, 108217.
17. Piekoszewski W., Szczerek M., Snarski-Adamski A.: Tribological characteristics of selected material pairs interacting in air and vacuum. Tribologia. 2018, 5, pp. 83–94.